



## Study on the Rheological Properties of CL-20/HTPB Casting Explosives

Hai-Xing LI, Jing-Yu WANG\* and Chong-Wei AN

*Chemical Industry and Ecology Institute, North University of China,  
Taiyuan 030051, China*

*\*E-mail: lihaixingabc@126.com*

**Abstract:** The rheological properties of  $\epsilon$ -2,4,6,8,10,12-hexanitro-2,4,6,8,10,12-hexaazaisowurtzitane (CL-20)/hydroxy-terminated polybutadiene (HTPB) casting explosives with different formulations were tested and analyzed. The effects of both the weight percentage (wt.%) of CL-20 and its particle size, as well as the type and content of plasticizers, on the rheological properties of CL-20/HTPB casting explosives were investigated in detail. The results show that the viscosity and pseudoplasticity of CL-20/HTPB casting explosives increase with increasing wt.% of CL-20 and decreasing particle size. The gradation of CL-20 particle size also affects the rheological properties of the casting explosives. When the mixing ratio of 30  $\mu\text{m}$  to 2  $\mu\text{m}$  particles is 3:1, the viscosity reaches its lowest value and the non-Newtonian index reaches the maximum value of 0.5698. The viscosity, non-Newtonian index and impact sensitivity of the samples studied are clearly decreased by the addition of dioctyl adipate (DOA), dioctyl sebacate (DOS) or dibutyl phthalate (DBP). However, the three plasticizers do not appear to affect the thermal decomposition of CL-20/HTPB casting explosives. With respect to the rheological properties, mechanical properties and sensitivity, DOA is the optimum plasticizer to use in CL-20/HTPB casting explosives.

**Keywords:** casting explosive, particle gradation, rheological properties, plasticizer

### 1 Introduction

Due to their good safety and mechanical properties, cast-cured explosives have been widely used in propellants and warhead charges [1-3]. Commonly, cast-cured explosives are composed of a polymeric binder with a high solids loading

of high explosive particles and some additives. Compared with compressed moulded explosives, cast-cured explosives are easier to fill into micro and complex structures due to their better flow characteristics. In the cast-cure process, the ingredients are mixed at ambient temperature to form a suspension that can be poured into containers and left to cure over time into a PBX explosive.

The explosive logic network and explosive synchronous network have been used in many explosive sequences [4-7]. Commonly, the network is composed of many small grooves, whose size is smaller than 1 mm×1 mm. In order to fill the casting composites into the small grooves, injection or extrusion processes were explored and introduced. In these moulding technologies, the rheological properties of the casting explosive directly affect the charging process and the properties of the charge in the small grooves.

Rheology is the science and technology of deformation of polymeric or plastic materials. Although the rheological properties of materials have been widely researched in many fields for a long time, the rheological properties of casting explosive have rarely been researched. The rheological properties of propellant suspensions, emulsion explosives and gel explosives had been investigated recently [8-13]. Many factors, such as the ratio of ingredients, temperature and cure time, affect the rheological properties of casting explosives. Nevertheless, more research should be conducted in this area, especially on the high solids loading formulations used in injection or extrusion processes. The present paper reports a systematic study of the effects of wt.% of CL-20 casting explosive, particle size and size gradations of CL-20, and the type and content of the plasticizers, on the rheological properties of the CL-20 casting explosives. The results may suggest ways for improving the extrusion or injection of CL-20 casting explosives.

## **2 Materials and Methods**

### **2.1 Materials**

The experimental materials are presented in Table 1.

**Table 1.** Experimental materials

Chemical name	Abbreviation	Property	Source
2,4,6,8,10,12-Hexa-nitro-2,4,6,8,10,12-hexaazaisowurtzitane	HNIW or CL-20	Raw CL-20: diameter of particles about 90 $\mu\text{m}$	Ordnance Industry Corporation 375 Factory
Hydroxy-terminated polybutadiene	HTPB	Molecular weight: about 2000 $\text{g}\cdot\text{mol}^{-1}$ and degree of functionality 2.28	Zibo Qilong Chemical Co., Ltd
Dioctyl adipate	DOA	Analytically pure	Tianjin Guangfu Fine Chemical Research Institute
Dioctyl sebacate	DOS	Analytically pure	Tianjin Guangfu Fine Chemical Research Institute
Dibutyl phthalate	DBP	Gas chromatography	Shanghai Jingchun Industrial Co., Ltd
Toluene diisocyanate	TDI	Analytically pure	Tianjin Dengke Chemical Reagent Co. Ltd

## 2.2 Methods

### 2.2.1 Preparation and scanning electron microscope (SEM) characterization of CL-20

Raw CL-20 particles were dissolved into ethyl acetate at ambient temperature to give a solution of concentration 0.3 g/mL. This was then filtered to remove insoluble material. When the CL-20 solution was dropped into the nonsolvent (n-heptane) at a rate of 1.5 mL/min, CL-20 particles, size about 30  $\mu\text{m}$ , were obtained. When the CL-20 solution was sprayed into the nonsolvent, using a sprayer with an air compressor at 0.5 MPa, CL-20 particles, size about 2  $\mu\text{m}$ , were obtained. The volume ratio of CL-20 solution to nonsolvent was 1:5. Finally, the fine CL-20 particles of the two sizes were filtered off by vacuum filtration and dried in a vacuum freeze drier.

The profiles of the CL-20 samples were characterized with a Hitachi S-4700 scanning electron microscope (SEM). SEM photographs of CL-20 with the different particle sizes are shown in Figure 1.

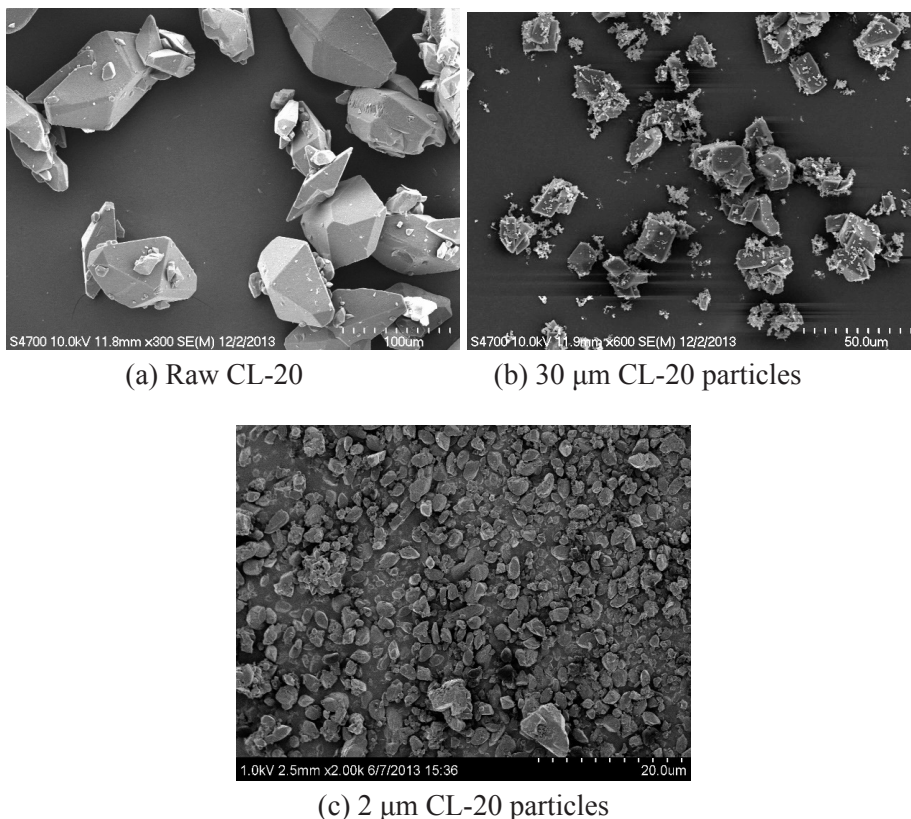


**Figure 1.** SEMs of CL-20 samples.

### 2.2.2 Formulations of the casting explosives

All formulations of the casting explosives are shown in Table 2. The casting explosive formulations were mixed at ambient temperature and pressure with a kneader. The mixing conditions were as follows: impeller speed 40 rpm, mixing time 20 minutes, the direction of rotation was changed once every 5 minutes.

For sample Nos. 1, 15, 18 and 19, 1 wt.% of toluene diisocyanate (TDI) was added to the cast explosive in the kneader at the end of the mixing process. After mixing, the composites were cast in a mould and then placed in a water bath oven at 50 °C for 7 days.

**Table 2.** Formulations of the casting explosives with different weight percentage of components

No.	CL-20 particles [wt.%]			HTPB [wt%]	DOA [wt.%]	DOS [wt.%]	DBP [wt.%]
	90 $\mu\text{m}$	30 $\mu\text{m}$	2 $\mu\text{m}$				
1	60	0	20	10	10	0	0
2	61.5	0	20.5	9	9	0	0
3	63	0	21	8	8	0	0
4	80	0	0	10	10	0	0
5	0	80	0	10	10	0	0
6	0	0	80	10	10	0	0
7	0	40	40	10	10	0	0
8	0	53.33	26.67	10	10	0	0
9	0	60	20	10	10	0	0
10	0	64	16	10	10	0	0
11	60	0	20	15	5	0	0
12	60	0	20	12	8	0	0
13	60	0	20	15	0	5	0
14	60	0	20	12	0	8	0
15	60	0	20	10	0	10	0
16	60	0	20	15	0	0	5
17	60	0	20	12	0	0	8
18	60	0	20	10	0	0	10
19	60	0	20	20	0	0	0

### 2.2.3 Characterization of the samples studied

The viscosity of all of the formulations was measured over a shear rate range of 0~100 s<sup>-1</sup> at 40 °C using a R/S rheometer (Brookfield).

The crystal phase of raw CL-20 and CL-20 in the cured samples Nos. 1, 15, 18 and 19 was determined by X-ray diffraction (XRD) analysis with a DX-2700 X-ray powder diffraction system (Dandong hao yuan company from China) using Cu-K $\alpha$  radiation at 40 kV and 30 mA. All samples were scanned from 10° to 50° with a step size of 0.03°.

The cured samples Nos. 1, 15, 18 and 19 were analyzed using a DSC-131 differential scanning calorimeter (Setaram company from France). The conditions of the DSC measurements were as follows: sample mass 0.5 mg; heating rate 15 °C/min; nitrogen atmosphere (flow rate 30 mL/min).

The impact sensitivity of the cured samples Nos. 1, 15, 18 and 19 was surveyed using a 12 type drop hammer apparatus according to the GJB-772A-97 standard method 601.2. The test conditions were: drop weight 5.000  $\pm$  0.002 kg;

sample mass  $35 \pm 1$  mg; temperature  $19^\circ\text{C}$  and relative humidity 50%. The results were based on tests on both sides of the 50% probability level using an up-and-down method. They were expressed as the critical drop-height of 50% explosion probability ( $H_{50}$ ) and standard deviation (S) [14].

### 3 Results and Discussion

#### 3.1 Crystal identification of CL-20 and CL-20 in the cast-cured explosives

Figure 2 shows the XRD patterns of raw CL-20 and the cured samples Nos. 1, 15, 18 and 19. This demonstrates that the crystal forms of raw CL-20 and CL-20 in the cast-cured explosives are all mainly of the  $\epsilon$ -form, and indicates that the mixing, casting and curing processes did not change the crystal morphology of the CL-20.

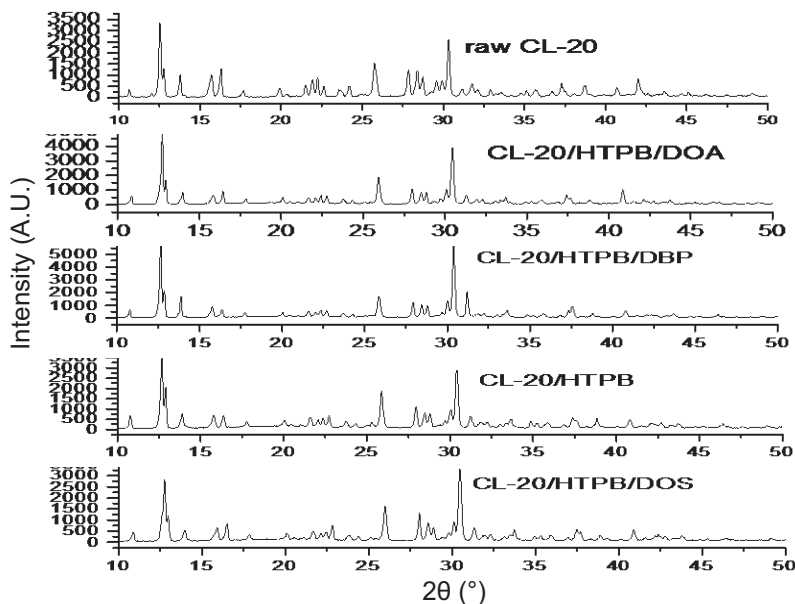


**Figure 2.** XRD patterns of raw CL-20 and CL-20 in the cast-cured explosives with different plasticizers.

### 3.2 Effect of wt.% of CL-20 on the rheological properties of the casting explosive

The study on the relation between viscosity ( $\eta$ ) and solid fraction ( $\phi$ ) has aroused much attention for a long time. Taking the maximum packing density ( $\phi_m$ ) into account can improve the predictive capability. The most common relationship is that proposed by Chong *et al.* [15]:

$$\eta_r = \left( 1 + 0.75 \frac{\phi / \phi_m}{1 - \phi / \phi_m} \right)^2 \quad (1)$$

where  $\eta_r$  is the relative viscosity, defined as the ratio of the suspension viscosity ( $\eta_s$ ) to the viscosity of the suspending medium ( $\eta_0$ ). It is known from Figure 3 that the viscosity increases with increasing solids loading, which is in line with Equation (1). The main reason for this is that the higher the solids content in a casting explosive is, the more frequently will the CL-20 particles collide with each other. In the collision process, energy dissipation is dominated by the relative movement of adjacent particles. Therefore, the viscosity of the CL-20 based casting explosive increases with increasing CL-20 content.

According to the definition of  $\phi_m$ ,  $\phi_m$  can represent the magnitude of the viscosity, where the viscosity tends to infinity when the solids fraction is close to  $\phi_m$ . As to how  $\phi_m$  is determined, an extensive analysis reveals that a linear relationship between  $1 - \eta_r^{-1/2}$  and  $\phi$  is frequently observed for a large variety of suspensions having sufficient solids content. Thus, the equation can be expressed as [16]:

$$1 - \eta_r^{-1/2} = a * \phi + b \quad (2)$$

Figure 4 shows the correlation between  $1 - \eta_r^{-1/2}$  and  $\phi$  and the fitting curves of Equation (2). The viscosity tends to infinity when the solids fraction is close to  $\phi_m$ , namely  $\eta_r^{-1/2} = 0$ . So Equation (2) is expressed as:

$$1 = a * \phi_m + b \quad (3)$$

Table 3 shows the computation of  $\phi_m$  based on Figure 4. From Table 3, a CL-20 casting explosive is about 93.5% of the maximum packing density.

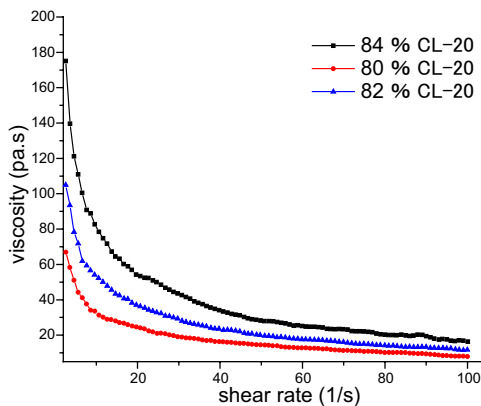


**Figure 3.**  $\eta - \dot{\gamma}$  correlation with different CL-20 solids fractions.

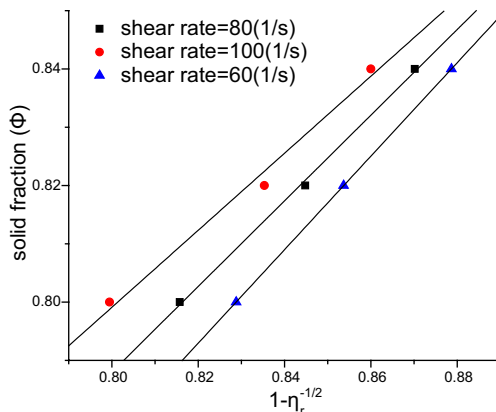


**Figure 4.** Linear relationship between  $\phi$  and  $1 - \eta_r^{-1/2}$ .

**Table 3.** Computation of  $\phi_m$  at shear rates of 60, 80 and 100 s<sup>-1</sup>

Shear rate (s <sup>-1</sup> )	Solids fraction ( $\phi$ )			Suspending medium (HTPB/DOA = 1:1)	$1 - \eta_r^{-1/2} = a * \phi + b$	$\phi_m = \frac{1-b}{a}$
	0.8	0.82	0.84			
	Viscosity (Pa.s)					
60	12.8246	17.5551	25.5361	0.3759	$a=1.2469, b=-0.1688$	0.937
80	10.0539	14.1776	20.2525	0.3414	$a=1.3610, b=-0.2724$	0.935
100	7.9192	11.7433	16.2465	0.3184	$a=1.513, b=-0.4091$	0.931

Figure 3 reveals that the viscosity of the CL-20 based casting explosive decreases as the shear rate is increased. This explains why a CL-20 based casting



explosive is a pseudoplastic fluid. According to Table 4, CL-20 based casting explosives also follow the power law model, namely:

$$\eta = K * \gamma^{n-1} \quad (4)$$

where  $K$  is a constant;  $\gamma$  is the shear rate;  $n$  is referred to as a non-Newtonian index. This suggests that a CL-20 based casting explosive is essentially a shear-thinning fluid. The shear-thinning behaviour indicates the presence of a connected particle network in these casting explosives [17]. Under sufficient shear, the particle network would break up into smaller flow units. The size of the flow units decreases with increasing shear force, which leads to shear-thinning behaviour. It is widely believed that shear thinning is due to the ordering of the particles into layers or strings which reduce the energy dissipation under shear [18].

Table 4 shows the power law model for different CL-20 contents. The pseudoplasticity of a CL-20 based casting explosive is enhanced and the non-Newtonian index is decreased with an increase in solids loading. If the viscosity of a casting explosive is excessively sensitive to shear rate, the rheological stability of the casting explosive will deteriorate because tiny fluctuations in the parameters in the charging process may cause a huge change in the rheological behaviour [19]. Decreases in the non-Newtonian index suggest that more flocculation has appeared in the sample. Extensive flocculation suggests that a network structure of the particles has developed and has become stronger by increasing the network connectivity and attraction between particles [20].

**Table 4.** Power law model with different CL-20 content

Solid fraction( $\phi$ )	$\eta = K * \gamma^{n-1}$	Correlation index
0.8	$K = 129.5219, n = 0.4261$	0.9982
0.82	$K = 228.875, n = 0.3725$	0.9990
0.84	$K = 373.0631, n = 0.343$	0.9990

An increase in solids loading can cause the yield value to increase [21, 22]. The higher the yield value is in a suspension, the stronger the particle network structure is [17], and a larger shear force is required to break up the network to cause flow. The magnitude of the yield value indicates the degree of difficulty for transition of the suspension from the static state to flow. To evaluate the yield stress ( $\tau_y$ ) of a casting explosive, a variety of models can be used which determine the yield stress from the  $\eta - \gamma$  curves (Figure 5 in this case) [21-23]. The yield value is usually calculated according to the Casson model [22] over a shear rate range of 1-20  $s^{-1}$ . It has the form:

$$\tau^{1/2} = \tau_y^{1/2} + c * \gamma^{1/2} \quad (5)$$

where  $\tau$  is the shear stress;  $\tau_y$  is the yield value;  $c$  is a constant;  $\gamma$  is the shear rate.

Figure 6 shows the Casson model curves of a CL-20 casting explosive. The linear relationship between  $\tau^{1/2}$  and  $\gamma^{1/2}$  can be clearly seen. Such linearity provides strong evidence for the presence of a connected particle network in these suspensions. As can be seen from Table 5, when the solids fraction is 0.8, 0.82 and 0.84, the yield value is 67.3192, 123.9737 and 202.4573 Pa, respectively. The yield value of a CL-20 based casting explosive increases with increasing solids loading.

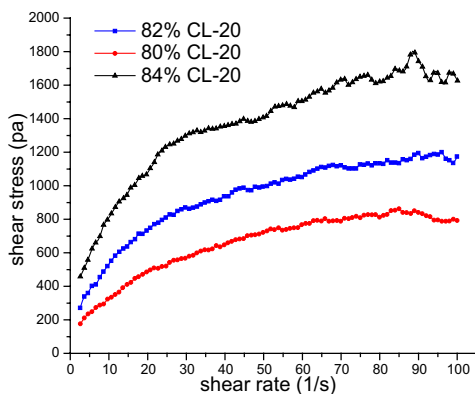


**Figure 5.**  $\tau - \gamma$  curves with different solid fractions.

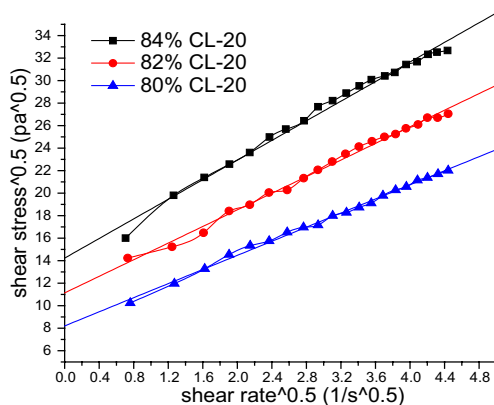


**Figure 6.** Fitting curves of the Casson model of CL-20 casting explosives with different solid fractions.

**Table 5.** Casson model of CL-20 casting explosives with different solid fractions

Solid fraction ( $\phi$ )	$\tau^{1/2} = \tau_y^{1/2} + c * \gamma^{1/2}$	Correlation index
0.8	$\tau_y = 67.3192, c = 3.1329$	0.9981
0.82	$\tau_y = 123.9737, c = 3.69$	0.9967
0.84	$\tau_y = 202.4573, c = 4.3566$	0.9945

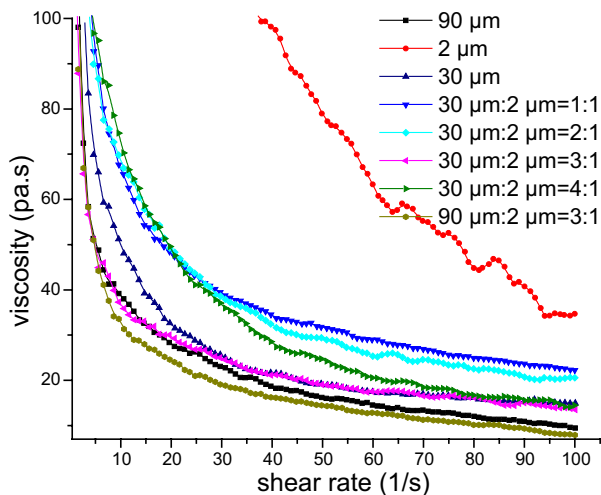
### 3.3 Effects of CL-20 particle size on the rheological properties of the casting explosive

Figure 7 shows the  $\eta - \gamma$  curves of CL-20 based casting explosive with different particle sizes and particle gradations. Comparing 90, 30 and 2  $\mu\text{m}$ , it can be seen that the viscosity decreases with an increase in the CL-20 particle size. Other studies have clearly confirmed that the value of  $\phi_m$  can be enhanced or reduced by altering the particle size distribution [24, 25]. Furthermore, the interaction between particles plays a crucial role in determining the rheological properties [17, 26-28]. Ogawa *et al.* theorized that viscosity increases with a decrease in particle size due to an increase in the overlapping areas of the electrical double layer around each particle [29]. It is also possible that the decrease in size of the CL-20 particles and the increase of surface protrusions and depressions lead to an increase in internal friction and inter-particle forces [30].

As for particle gradation, it is crucial to control the following two process parameters: (i) ratio of the diameters of large to fine particles, namely  $\lambda$ ; (ii) the relative content of fine particles, namely  $\zeta$ . For constant solids loading, tests have shown that the viscosity is significantly reduced when  $\lambda$  increases from 1 to 7.25. But when  $\lambda$  is more than 10, the viscosity of the suspension does not decrease further with increasing  $\lambda$  [15]. Academic scholars believe that particle gradation is better utilised when  $\lambda = 6.45$  and  $\zeta \approx 25\%$  [31]. As can be seen from Figure 7, when 30  $\mu\text{m}$  CL-20 particles are mixed in different proportions with 2  $\mu\text{m}$  particles, the viscosity with a mixing ratio of 3:1 is lower than the viscosity with mixing ratios of 1:1, 2:1 and 4:1, and even lower than the viscosity with 30  $\mu\text{m}$  particles alone. Similarly, when 90  $\mu\text{m}$  particles are mixed with 2  $\mu\text{m}$  particles, the viscosity with a mixing ratio of 3:1 is also lower than the viscosity with 90  $\mu\text{m}$  particles alone. Therefore, a mixing ratio of 3:1 of large to fine particles is the best particle gradation.

According to Table 6, the fitting parameters are obtained through the fitting of the power law model. It can be seen that the non-Newtonian index increases with a decrease in the CL-20 particle size. As for particle gradation, when the mixing ratio of 30  $\mu\text{m}$  CL-20 particles to 2  $\mu\text{m}$  particles is 3:1, the non-Newtonian index reaches the maximum value of 0.5698. Therefore, a CL-20

casting explosive with a mixing ratio of 3:1 of large to fine particles can ensure flow stability in the charging process.



**Figure 7.**  $\eta - \dot{\gamma}$  curves of CL-20 casting explosives with different particle sizes and particle gradations.

**Table 6.** Power law model with different particle sizes and particle gradations

Particle size and particle gradation	$\eta = K * \dot{\gamma}^{n-1}$	Correlation index
2 $\mu\text{m}$	$K = 907.7151, n = 0.349$	0.9891
30 $\mu\text{m}$ : 2 $\mu\text{m}$ = 1:1	$K = 184.0169, n = 5471$	0.9998
30 $\mu\text{m}$ : 2 $\mu\text{m}$ = 2:1	$K = 200.7336, n = 5062$	0.9989
30 $\mu\text{m}$ : 2 $\mu\text{m}$ = 3:1	$K = 103.5669, n = 0.5698$	0.9993
30 $\mu\text{m}$ : 2 $\mu\text{m}$ = 4:1	$K = 281.8724, n = 0.3708$	0.9956
30 $\mu\text{m}$	$K = 166.79, n = 0.4285$	0.9989
90 $\mu\text{m}$ : 30 $\mu\text{m}$ = 3:1	$K = 128.2954, n = 0.4578$	0.9914
90 $\mu\text{m}$	$K = 136.8621, n = 0.4506$	0.9984

### 3.4 Effect of plasticizers on the rheological properties of CL-20 casting explosives

#### 3.4.1 The effect of the weight percentage of individual plasticizers on the rheological properties.

Figure 8 shows the  $\eta - \dot{\gamma}$  curves of CL-20 casting explosives with different plasticizer contents. Viewing the plasticizing effect of three plasticizers, it is

observed that all three plasticizers can largely reduce the viscosity of CL-20 based casting explosives. However, the degree of viscosity decrease is reduced with increasing plasticizer content. Commonly, the plasticizer is a kind of additive having a low molecular weight, high boiling point and low volatility, and can be mixed with the polymer. Intermolecular interactions exist between the macromolecular chains of the polymer. The viscosity of a suspension is connected to the molecular structure of the polymer. The adhesive forces between the molecules creates a certain strength to the polymer and also affect its processing performance. Plasticizers interspersed between the polymer molecules can weaken the intermolecular forces, which improves the processability and flexibility of the polymer due to the increase in activity of the polymer molecules [32].

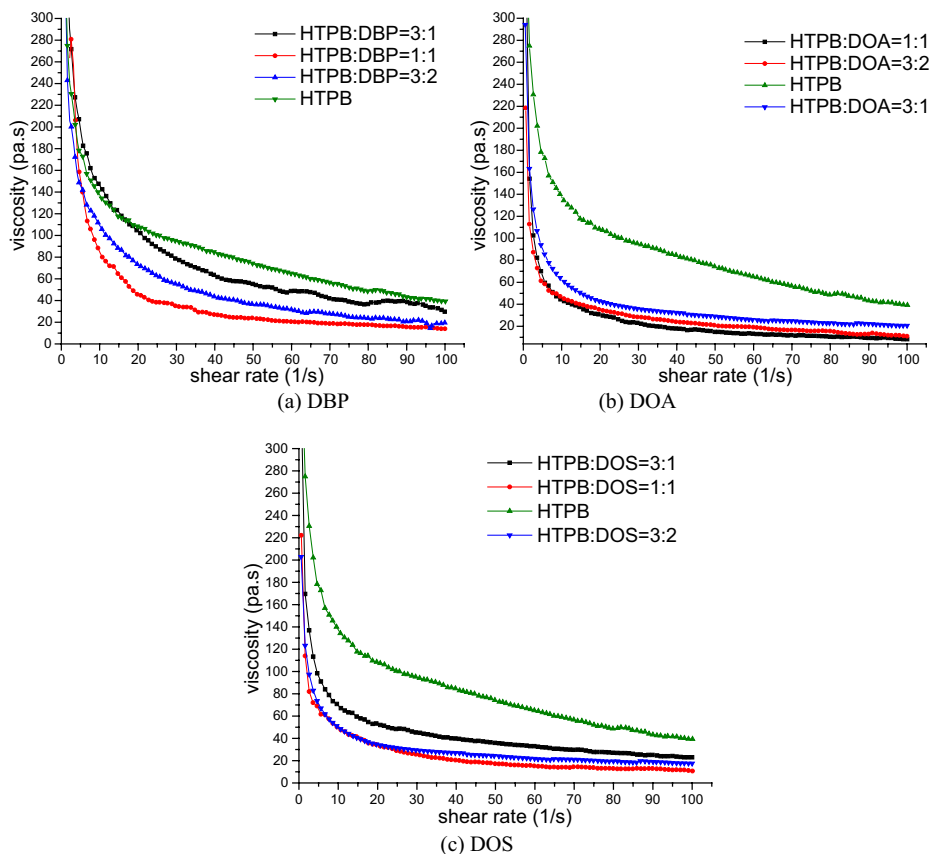


**Figure 8.**  $\eta - \dot{\gamma}$  curves of CL-20 casting explosives with different plasticizer contents.

### 3.4.2 Effect of plasticizer type on the rheological properties

Figure 9 shows the  $\eta - \dot{\gamma}$  curves of CL-20 based casting explosives with different plasticizers. It is observed that the viscosity of the casting explosive containing DOA is the lowest, whilst DOS ranks second. Therefore, the plasticizing effect of DOA is the best of the types studied with respect to viscosity. This might be due to the molecular structure of DBP with its macromolecular benzene rings, making flowing of the DBP molecules more difficult than the other two plasticizers which have no benzene rings. The DOA molecule is substantially a straight chain molecule with short branches and has a low molecular weight, while the molecular structure of DOS tends to a triangular shape and the DOS molecule is heavier than the DOA molecule. Therefore DOA molecules are easier to flow, leading to the plasticizing effect of DOA being better than DOS [33].

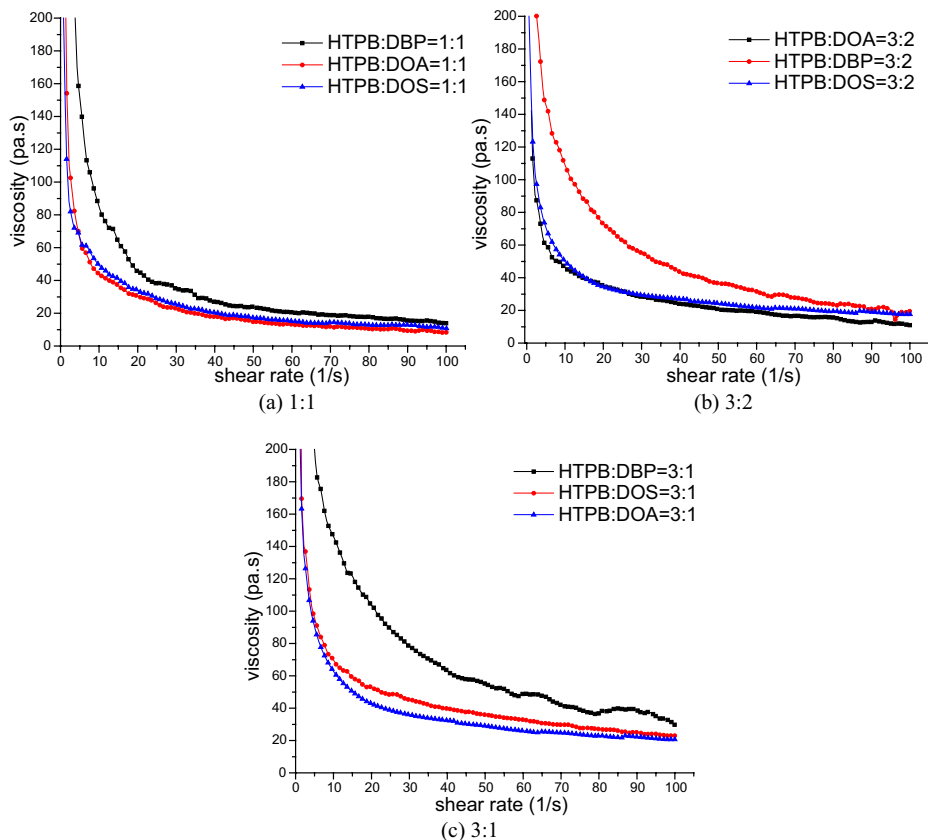


**Figure 9.**  $\eta - \dot{\gamma}$  curves of CL-20 casting explosives with different ratios of HTPB to plasticizers.

From the power law model, Table 7 shows the fitting parameters of CL-20 based casting explosives with different plasticizer types and contents in the binder. From Table 7, it can be seen that the non-Newtonian index increases with an increase in the plasticizer content in the binder when the same plasticizer is used. For different plasticizers, when the ratio of plasticizer to HTPB is constant, the non-Newtonian index of the casting explosive using DOS is the largest, which indicates that the non-Newtonian index of the casting explosive using DOS is least reduced and the DOA plasticizer ranks second. Although the three plasticizers can greatly reduce the viscosity of the suspension, they can also enhance the pseudoplasticity of the casting explosives. However, relatively speaking, the pseudoplasticity of the casting explosive with DOS is the weakest, which favours rheological stability in the charging process.

**Table 7.** Fitting parameters of the power law model of CL-20 casting explosives with different plasticizers and plasticizer contents

Plasticizer/ HTPB	HTPB-DOA	HTPB-DOS	HTPB-DBP
0	$K = 408.7313, n = 0.5372$		
1:3	$K=204.2564, n=0.49$	$K=220.7327, n=0.5241$	$K=535.3215, n=0.4136$
2:3	$K=168.5252, n=0.4532$	$K=153.8584, n=0.515$	$K=468.3176, n=0.3141$
1:1	$K=229.8205, n=0.3015$	$K=183.0734, n=0.4026$	$K=537.1744, n=0.2058$

### 3.4.3 Effect of plasticizer type on thermal decomposition

The DSC curves of the cured samples nos. 1, 15, 18 and 19 are shown in Figure 10. It can be seen that the DSC curves of CL-20/HTPB casting explosives have two exothermic peaks: the HTPB exothermic peak and the CL-20 decomposition peak. It is observed that there is little difference among the peak temperatures of the four formulations. The three plasticizers all increase the CL-20 decomposition peak temperature slightly and decrease the HTPB peak temperature, except for DBP which decreases the CL-20 decomposition peak temperature. Thus, they do not obviously affect the thermal decomposition of CL-20 based cast-cured explosives. Of the samples studied the formulation with DOA has the highest CL-20 decomposition peak temperature.

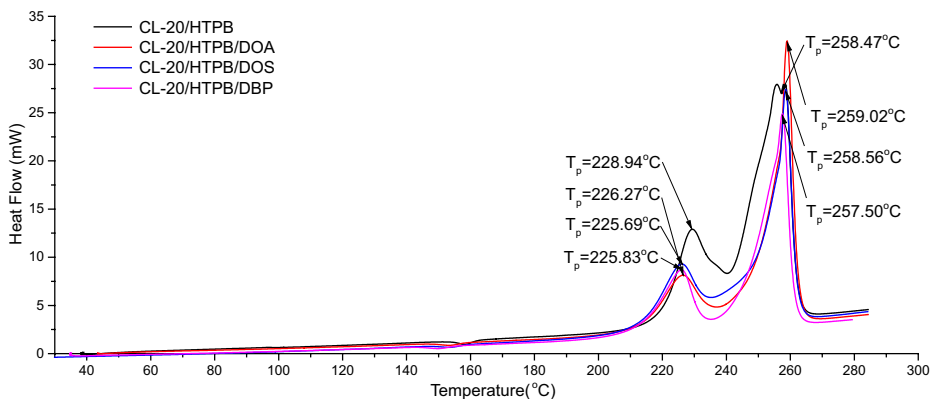


**Figure 10.** DSC curves of CL-20 based cast-cured explosives with different components at 15 °C/min heating rate.

#### 3.4.4 Effect of plasticizer type on the impact sensitivity

The impact sensitivities of cured samples are listed in Table 8. It can be seen that all three plasticizers increase the drop height ( $H_{50}$ ) of CL-20 based cast-cured explosives. The drop height of the CL-20 based cast-cured explosive with DBP is nearly three times that of the formulation without plasticizer. The results suggest that CL-20 based cast-cured explosives with DBP or DOA are difficult to explode with an impact stimulus and exhibit insensitive characteristics.

**Table 8.** Impact sensitivity of cured samples

Cured samples	Drop height $H_{50}$ /cm	Standard deviation/ $\sigma$
CL-20/HTPB/TDI	20.7	0.085
CL-20/HTPB/DOA/TDI	54.5	0.0761
CL-20/HTPB/DOS/TDI	41.2	0.088
CL-20/HTPB/DBP/TDI	61.1	0.0895

## 4 Conclusions

This paper has investigated in detail the rheological properties of CL-20/HTPB casting explosives with different formulations. The weight percentage of CL-20 and its particle size, in addition to the type and weight percentage of plasticizer, affected the rheological properties of CL-20/HTPB casting explosives. CL-20 based casting explosives exhibited pseudoplasticity. The viscosity, yield value and pseudoplasticity increased with an increase of the CL-20 content and a decrease



of CL-20 particle size. As for the particle gradation, when the mixing ratio of large to fine particles was 3:1, the casting explosive reached the lowest viscosity with the largest non-Newtonian index. The plasticizers DOA, DOS and DBP all dramatically reduced the viscosity of the casting explosives. The viscosity was reduced with increasing plasticizer content while the pseudoplasticity was the reverse. Moreover, the casting explosives with plasticizers had lower impact sensitivity than that of the formulation without plasticizer. The three plasticizers had no significant effect on the decomposition temperature of the CL-20 casting explosives. With respect to the rheological properties, mechanical properties and sensitivity, DOA should be the best plasticizer of the types studied.

## 5 References

- [1] Agrawal J.P., Some New High Energy Materials and Their Formulations for Specialized Applications, *Propellants Explos. Pyrotech.*, **2005**, 30(5), 316-328.
- [2] Lee J.S., Hsu C.K., Thermal Properties and Shelf Life of HMX-HTPB Based Plastic-bonded Explosives, *Thermochim. Acta*, **2002**, 392, 153-156.
- [3] Luo G., Huang H., Zhang M., Guan L.F., Li S.B., Study on Low Vulnerability of Cast-cured PBX Aluminized Explosive, *Energ. Mater.*, **2004**, 12(1), 20-22.
- [4] Jiang D.C., Sun C.W., Zeng F.Q., Yang B., Studies on Explosive Logic Network of Sixpartite Circle, *Explosion and Shock Waves*, **1997**, 17(3), 228-236.
- [5] Ji L.G., Feng C.G., Cai R.J., Jiao Q.J., Development of Explosive Technique for Explosive Logic Network, *Initiators Pyrotech. (Huogongpin)*, **1996**, 4, 29-33.
- [6] Wen Y.Q., Jiao Q.J., A Study on the Precision Press Loading Technique of a Synchronous Multi-point Explosive Circuit, *Acta Armamentarii (Binggong Xuebao)*, **2006**, 27(3), 005.
- [7] Zheng Y., Wang X.M., Huang Y.S., Li W.B., Li W.B., Design and Experimental Investigation on Multi-point Synchronous Explosive Logic Circuit, *Initiators Pyrotech. (Huogongpin)*, **2008**, 1, 1-4.
- [8] Kalyon D.M., Yaras P., Aral B., Yilmazer U., Rheological Behavior of a Concentrated Suspension: a Solid Rocket Fuel Simulant, *J. Rheol.*, **1993**, 37(1), 35-53.
- [9] Miller R.R., Lee E., Powell R.L., Rheology of Solid Propellant Dispersions, *J. Rheol.*, **1991**, 35(5), 901-920.
- [10] Mudeme S., Masalova I., Haldenwang R., Kinetics of Emulsification and Rheological Properties of Highly Concentrated Explosive Emulsions, *Chemical Engineering and Processing: Process Intensification*, **2010**, 49(5), 468-475.
- [11] Lu S.Y., Shao Z.Q., Wang F.J., Zhang Y.D., Zhang Z.L., Preparation of New Energetic Gelator and Rheological Properties of Its Gel, *Chin. J. Explos. Propellants (Huozhayao Xuebao)*, **2011**, 34(1), 49-53.
- [12] Zhang W., Fan X.Z., Chen Y.D., Xie W.X., Liu Z.R., Wei H.J., Rheological Study

- on the Crosslinking of NEPE Propellant, *Chemical Journal of Chinese Universities (English Edition)*, **2009**, 30(6), 1230-1234.
- [13] Zhang D.J., Zhang X.T., Lu L.Y., Zhang J.Y., Study on Influence of Oily Material on Emulsion Matrix Viscosity of On-site Mixing Explosive, *Initiators Pyrotech. (Huogongpin)*, **2013**, 1(1), 42-45.
- [14] National Military Standard of China, *Experimental Methods of Sensitivity and Safety* (in Chinese), *GJB/772A-97*, **1997**.
- [15] Chong J.S., Christiansen E.B., Baer A.D., Rheology of Concentrated Suspensions, *J. Appl. Polym. Sci.*, **1971**, 15(8), 2007-2021.
- [16] Liu D.M., Particles Packing and Rheological Property of Highly-concentrated Ceramic Suspensions:  $\phi_m$  Determination and Viscosity Prediction, *J. Mater. Sci.*, **2000**, 35(21), 5503-5507.
- [17] Chang J.C., Lange F.F., Pearson D.S., Viscosity and Yield Stress of Alumina Slurries Containing Large Concentrations of Electrolyte, *J. Am. Ceram. Soc.*, **1994**, 77(1), 19-26.
- [18] Hoffman R.L., Explanations for the Cause of Shear Thickening in Concentrated Colloidal Suspensions, *J. Rheol.*, **1998**, 42(1), 111-123.
- [19] Wang J.H., Shi Q.N., Xi J., Research on Critical Powder Loading for Ti-6Al-4V Alloy Feedstocks, *Hot Working Technolog.*, **2012**, 41(5), 11-13.
- [20] Liu D.M., Rheology of Aqueous Suspensions Containing Highly Concentrated Nano-sized Zirconia Powders, *J. Mater. Sci. Lett.*, **1998**, 17(22), 1883-1885.
- [21] Dzuy N.Q., Boger D.V., Yield Stress Measurement for Concentrated Suspensions, *J. Rheol.*, **1983**, 27(4), 321.
- [22] Dash R.K., Mehta K.N., Jayaraman G., Casson Fluid Flow in a Pipe Filled with a Homogeneous Porous Medium, *Int. J. Eng. Sci.*, **1996**, 34(10), 1145-1156.
- [23] Keentok M., The Measurement of the Yield Stress of Liquids, *Rheol. Acta*, **1982**, 21(3), 325-332.
- [24] Mewis J., Spaul A.J.B., Rheology of Concentrated Dispersions, *Adv. Colloid Interface Sci.*, **1976**, 6(3), 173-200.
- [25] Edirisinghe M.J., Evans J.R.G., Review: Fabrication of Engineering Ceramics by Injection Moulding.I. Materials Selection, *Int. J. High Technol. Ceram.*, **1986**, 2(1), 1-31.
- [26] Lange F.F., Powder Processing Science and Technology for Increased Reliability, *J. Am. Ceram. Soc.*, **1989**, 72(1), 3-15.
- [27] Bergström L., Schilling C.H., Aksay I.A., Consolidation Behavior of Flocculated Alumina Suspensions, *J. Am. Ceram. Soc.*, **1992**, 75(12), 3305-3314.
- [28] Yanez J.A., Shikata T., Lange F.F., Pearson D.S., Shear Modulus and Yield Stress Measurements of Attractive Alumina Particle Networks In Aqueous Slurries, *J. Am. Ceram. Soc.*, **1996**, 79(11), 2917-2917.
- [29] Ogawa A., Yamada H., Matsuda S., Okajima K., Doi M., Viscosity Equation for Concentrated Suspensions of Charged Colloidal Particles, *J. Rheol.*, **1997**, 41(3), 769-785.
- [30] Pang W.Q., Fan X.Z., Xu H.X., Rheological Properties of Agglomerated Boron

- Particles in the HTPB-based Fuel-rich Propellant, *Chin. J. Explos. Propellants (Huozhayao Xuebao)*, **2010**, 33(3), 84-87.
- [31] Li B.S., Jiang H.Y., Li Z.Q., Fan H.B., An G.Y., Effect of Bipeak Grain-size Distribution of  $ZrO_2$  Powder on Viscosity of Coating in Ti-alloy Investment Casting, *Foundry*, **1999**, (6), 22-24.
- [32] Shi F.C., Shi Z.B., Jiang P.P., *Plasticizer and Its Application*, Vol.1, Chemical Industry Press, Beijing, **2002**, pp. 1-2.
- [33] Gao L.L., Xi P., Application of ATP-28 in Cast-cured Explosive, *Chin. J. Energ. Mater. (Hanneng Cailiao)*, **2008**, 16(6), 689-692.

